Bioactive Materials 45 (2025) 509–519

Contents lists available at ScienceDirect

Bioactive Materials

journal homepage: www.keaipublishing.com/en/journals/bioactive-materials

Local delivery of TGF-β1-mRNA decreases fibrosis in osteochondral defects

Gianluca Fontana [a], Brett Nemke [b], Yan Lu [b], Connie Chamberlain [a], Jae-Sung Lee [a], Joshua A. Choe [a], Hongli Jiao [a], Michael Nelson [a], Margot Amitrano [a], Wan-Ju Li [a], Mark Markel [b], William L. Murphy [a,c,d,*]

[a] Department of Orthopedics and Rehabilitation, USA
[b] School of Veterinary Medicine, USA
[c] Department of Biomedical Engineering, USA
[d] Material Sciences and Engineering, University of Wisconsin-Madison, Madison, WI, USA

ARTICLE INFO

Keywords:
Cartilage
Fibrocartilage
mRNA delivery
Gene therapy
Microparticles

ABSTRACT

Osteoarthritis (OA) is a condition that affects the quality of life of millions of patients worldwide. Current clinical treatments, in most cases, lead to cartilage repair with deposition of fibrocartilage tissue, which is mechanically inferior and not as durable as hyaline cartilage tissue. We designed an mRNA delivery strategy to enhance the natural healing potential of autologous bone marrow aspirate concentrate (BMAC) for articular cartilage repair. We used mineral-coated microparticles to deliver TGF-β1 mRNA to autologous BMAC. mRNA-activated BMAC was suspended in peripheral blood to generate therapeutic BMAC clots, which were then implanted in rabbit osteochondral defects. Tracking studies revealed that the clots were reliably maintained in the defects for at least 2 weeks. TGF-β1 mRNA delivery significantly increased TGF-β1 production in BMAC clots and increased early expression of articular chondrocyte markers within osteochondral defects. At 9 weeks post-surgery, the mRNA-treated defects had a superior macroscopic cartilage appearance, decreased type I collagen deposition, increased stain intensity for type II collagen and increased glycosaminoglycan deposition area when compared to the controls. Despite the transient expression of therapeutic mRNA we have detected lasting effects, such as a decrease in fibrocartilage formation demonstrated by the decrease in type I collagen deposition and the improvement in macroscopic appearance in the treatment group.

1. Introduction

Osteoarthritis (OA) and its associated cartilage degeneration, affect more than 240 million people worldwide [1]. OA patients usually experience reduced mobility and pain, and they require frequent healthcare services for an average of 26 years per patient [2]. Thus, OA erodes the quality of life of millions of patients and causes considerable social expenditure [3]. Moreover, owing to aging demographics and an increasingly sedentary lifestyle, OA is expected to become the most common musculoskeletal disease by 2040 [3]. Despite the prevalence of OA, current treatments are primarily palliative and do not prevent further cartilage degeneration. Articular cartilage is comprised of predominately type II collagen, is avascular, and has a limited ability to regenerate [4]. Physiological repair is hampered by low cellularity and a diffusion-limited supply of nutrients and oxygen [5]. It is challenging to design tissue engineering strategies to regenerate cartilage because there are gaps in our knowledge of how cartilage degenerates and to what extent it can regenerate [5].

One approach that has been tested for cartilage regeneration is the implantation of bone marrow-derived mesenchymal stromal cells (BM-MSCs) [6]. Although BM-MSCs can potentially differentiate into chondrocytes [7], they have significant biological limitations that prevent them from being approved for clinical use [8]. For instance, when BM-MSCs are expanded *in vitro*, they are exposed to abnormally high oxygen levels, which primes them to produce type I collagen even after undergoing full chondrogenic differentiation [9,10]. When *in vitro*-expanded BM-MSCs were implanted into cartilage defects *in vivo,* they were shown to induce type I collagen synthesis and promote osteochondral ossification [11,12]. Moreover, strategies proposing the transplantation of *in vitro* expanded BM-MSCs are likely to be subject to

Peer review under the responsibility of KeAi Communications Co., Ltd.
* Corresponding author. Department of Orthopedics and Rehabilitation, USA.
E-mail address: wlmurphy@ortho.wisc.edu (W.L. Murphy).

https://doi.org/10.1016/j.bioactmat.2024.11.033
Received 23 September 2024; Received in revised form 25 November 2024; Accepted 27 November 2024

complex regulations for clinical use because their expansion constitutes a significant manipulation of the cells [13]. The use of autologous tissue can potentially provide a simpler alternative approach for clinical cartilage regeneration.

Several studies have reported that full-thickness cartilage defects tend to heal better than superficial defects, highlighting the potential contributory role of bone marrow cells migrating from the subchondral bone [14,15]. For this reason, microfracture and subchondral drilling are techniques that are currently used clinically to treat cartilage defects. However, the resulting cartilage has poor biomechanical properties, and the neo-cartilage structure resembles fibrocartilage rather than hyaline cartilage [16]. An alternative approach to deliver autologous bone marrow-derived cells to a cartilage defect involves harvesting and delivering bone marrow aspirate concentrate (BMAC). A study found a clear correlation between BMAC cellularity and improved clinical outcomes [17], suggesting that the cells in the BMAC can engage in neo-cartilage formation. In addition, BMAC contains growth factors and anti-inflammatory proteins that can influence tissue regeneration [6]. However, clinical reports have shown that while BMAC implantation has low-risks [18,19] and facilitates fibrocartilage repair, it is insufficient to prompt hyaline cartilage regeneration [16]. In fact, implantation of BMAC alone may lead to poor long-term outcomes, due in large part to the formation of fibrocartilage [16,20,21].

One of the main hallmarks of fibrocartilage formation is the shift in collagen deposition from type II to type I. This shift has negative consequences for cartilage quality from structural, functional, and biological perspectives. The increase in collagen I deposition alters the physico-chemical properties of cartilage ECM; this, in turn, affects nutrient diffusion and the ability of cartilage to maintain homeostasis [6]. On the other hand, the loss of type II collagen observed in fibrocartilage can disrupt the physiological microenvironment of chondrocytes. When collagen II levels decrease, chondrocytes may receive altered mechanical and biochemical signals from the ECM, causing phenotypic changes [5]. Finally, fibrocartilage has inferior compressive stiffness under load, and it wears more rapidly than hyaline cartilage [22]. For these reasons, maintaining high concentrations of type II collagen and low concentrations of type I collagen is important for the homeostasis of cartilage. Here, we aimed to increase the therapeutic potential of BMAC by co-delivering mRNA encoding for TGF-β1. We chose to use this approach rather than the delivery of recombinant protein because in a recent study we have demonstrated that under appropriate conditions, mRNA delivery can induce long-lasting biological responses *in vivo* [23]. We found that the biological effects obtained via mRNA delivery surpassed those achieved through the delivery of recombinant proteins [23]. We hypothesized that co-delivery of BMAC and TGF-β1-mRNA will support neo-cartilage formation and decrease fibrocartilage formation, as TGF-β1 is a well-established anabolic mediator of cartilage formation [24]. We used mineral-coated

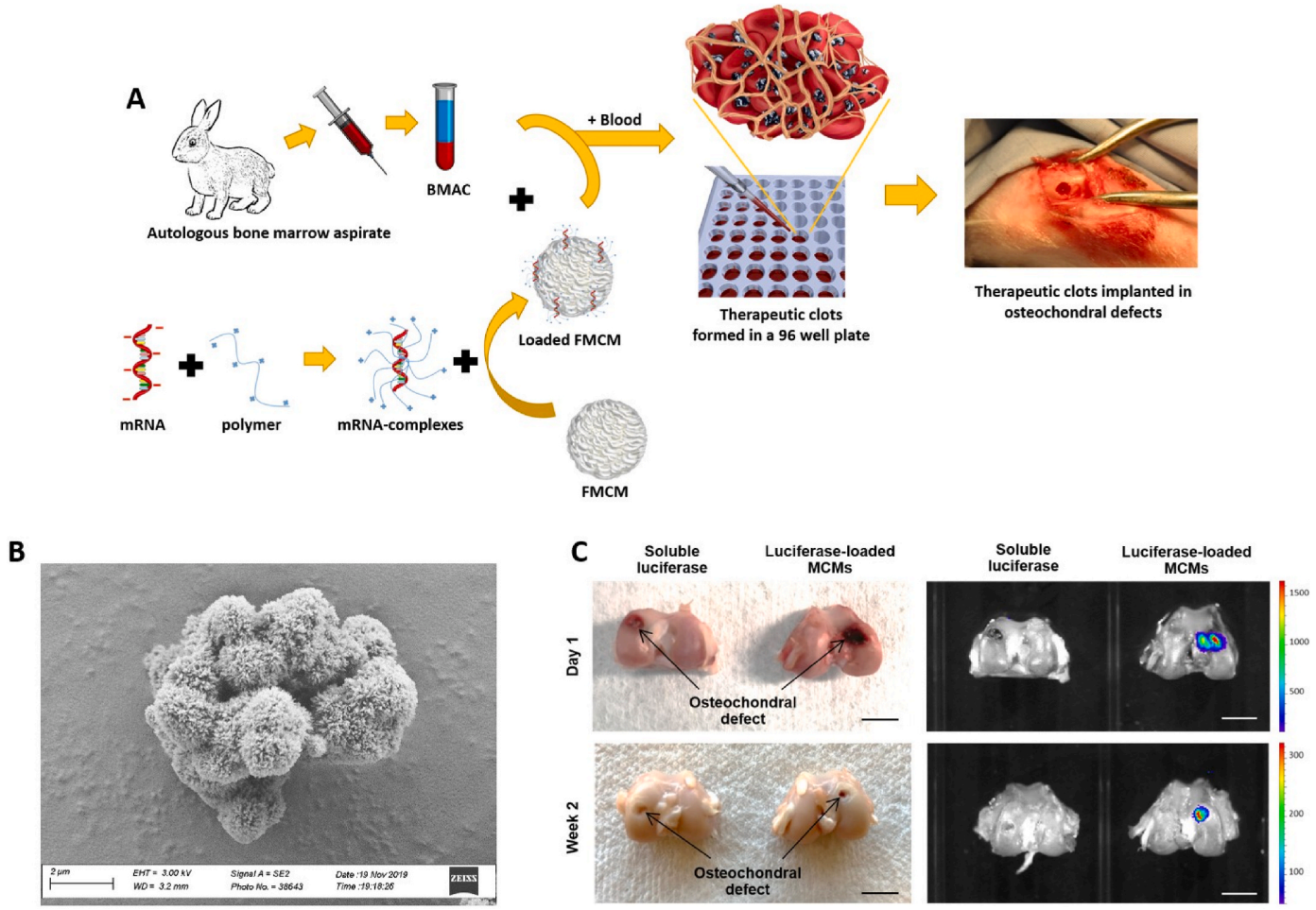

Fig. 1. BMAC clots are stable for 2 weeks in vivo. (**A**) Schematic representation of the procedure to manufacture BMAC clots. mRNA is complexed with a polymeric complexing agent, the mRNA complexes are then loaded on FMCM. In the meantime bone marrow aspirates are harvested from rabbits and the cells are concentrated to obtain BMAC. Loaded FMCM and BMAC are mixed briefly in a 96 well plate. The well is then filled with peripheral blood and let clot for 5 min. The BMAC clots are then implanted in osteochondral defects. Scalebar = 5 mm. (**B**) Scanning electron micrograph of FMCMs, scalebar = 2 μm. (C) Images of osteochondral defect explants with relative bioluminescent images reveal that clots loaded with FLUC-MCM are still within the defects 14 days post-surgery. Scalebar = 5 mm.

microparticles (MCMs) to deliver mRNA, as our recent studies have shown that MCMs can significantly decrease cytotoxicity while enabling higher levels of local mRNA transfection [25]. Moreover, we previously showed that MCMs can sequester, stabilize, and release proteins encoded by the delivered mRNA, enhancing their biological activity [23]. In the current study, therapeutic BMAC was combined with mRNA-loaded MCMs and encapsulated in autologous peripheral blood clots to form a matrix for neo-tissue formation, and the resulting clots were implanted into a rabbit osteochondral defect (Fig. 1A).

2. Materials and methods

2.1. In vitro

2.1.1. Synthesis of mineral coated microparticles

β-Tricalcium phosphate (β-TCP) 2 μm powder (Cam Bioceramics) was used as a microparticle core material. The β-TCP was incubated in regular modified simulated body fluid (mSBF) at concentration of 1 mg/mL for a total of 7 days. The regular mSBF solution for the synthesis of regular MCM was prepared at pH 6.8 using 141 mM NaCl, 4 mM KCl, 0.5 mM $MgSO_4$, 1 mM $MgCl_2$, 4.2 mM $NaHCO_3$, 20 mM HEPES, 5 mM $CaCl_2$, 2 mM KH_2PO_4. A version of MCM doped with fluoride (FMCM) were prepared by adding 1 mM NaF to the regular mSBF solution. The suspension was rotated at 37 °C. Every 24 h for 7 days, the microparticles were centrifuged at 2,000g for 5 min, and the supernatant was discarded and replaced with freshly made mSBF. After 7 days, resulting MCMs were washed three times with 50 mL deionized water and filtered through a 40 μm pore cell strainer. The MCM were then concentrated by centrifugation and lyophilized for 48 h.

2.1.2. Synthesis of TGF-β1-encoding mRNA

The transcript coding sequence for ransforming growth factor beta 1 (TGF-β1) (Gene ID: 7040) was obtained from the National Center for Biotechnology Information. pDNA for TGF-β1 was synthesized by cloning custom dsDNA (Integrated DNA Technologies) with Gibson Assembly (New England Biolabs) into a backbone plasmid containing 5′ and 3′ untranslated regions from the β-Globin Gene. High fidelity PCR (New England Biolabs) with a 3' primer appended 120 nt poly-dT tail was used to generate double stranded DNA templates. mRNA was produced by *in vitro* transcription with co-transcriptional capping (anti-reverse cap analogue; New England Biolabs), incorporation of chemically modified nucleotides, 5-methylcytidine and pseudouridine (TriLink Biotechnologies). mRNA was purified using spin-columns (New England Biolabs).

2.1.3. Characterization of TGF-β1-encoding mRNA

The concentration of TGF-β1-mRNA was measured spectrophotometrically while the size was determined via 1 % agarose gel with 1 % bleach. The TGF-β1-mRNA was stored at −80 °C. The assessment of the mRNA expression product was conducted using a cell-free assay. This enabled us to reduce background due to the presence of TGF-β1 in the serum generally used in cell culture media. The mRNA was translated by a cell-free rabbit reticulocyte lysate system (Promega) and the TGF-β1 quantified by ELISA specific for human TGF-β1 (R&D Systems).

2.1.4. Cell culture

Rabbit BMAC was cultured *in vitro* for 2 days in Iscove's modified Dulbecco's media (IMDM) containing: 10 % human serum type AB (Access Cell Culture), 1X non-essential amino acids (Fisher Scientific), 4 mM L-glutamine (Fisher Scientific), 1 mM sodium pyruvate (Thermo Fisher Scientific), 4 μg/mL human insulin (Sigma Aldrich) and 1 % penicillin and streptomycin (P/S). Alternatively, BMAC was also cultured in RPMI media (Corning) containing 10 % fetal bovine serum (FBS) or in raw bone marrow (Not processed and collected in EDTA-coated tubes).

2.1.5. Preparation of mRNA complexes with MCMs

We utilized TGF-β1-mRNA and firefly luciferase (FLUC) mRNA for our studies. The FLUC mRNA employed was optimized for mammalian systems, polyadenylated, and modified with 5-methoxyuridine (TriLink). The formation of mRNA complexes involved either a polymeric complexing agent, TransIT® (Mirus Bio), or a lipidic complexing agent, MessengerMax™ (ThermoFisher Scientific). To synthesize mRNA complexes, the mRNA was resuspended in Optimem to achieve a final concentration of 15 μg/mL. For mRNA-lipid complexes, 1 μL of MessengerMax was added per 1 μg of mRNA, while for mRNA-polymer complexes, 2 μL of Booster reagent and 2 μL of TransIT reagent were added per μg of mRNA. The mRNA complexes were allowed to form at room temperature for 5 min. Loading of the mRNA complexes onto MCM or FMCM was achieved by resuspending 375 μg of microparticles for every μg of mRNA in solution and incubating for 1 h at room temperature. The loaded microparticles were collected by centrifugation and resuspended in Optimem.

2.1.6. Cell transfection with mRNA/MCM complexes (in vitro)

We optimized the transfection conditions *in vitro* before delivering mRNA *in vivo*. For the *in vitro* part: the day before the transfection we seeded 10,000 cells per well (Rabbit BMAC) in a 96-well plate. The transfection was obtained by transferring the mRNA-MCM solution described above so to have 200 ng of complexed mRNA in each well. To have consistency in the transfection rate, mRNA complexes were prepared immediately before each experiment and the outcomes of transfection measured after 24 h.

2.2. In vivo

2.2.1. Animal models

All procedures involved in the animal study were approved by the University of Wisconsin-Madison Institutional Animal Care and Use Committee (approval number: V006006-R02). During all surgeries we tried to minimize animals suffering. For the osteochondral defect model and for harvesting bone marrow we used a total of 60 New Zealand White Rabbits. All rabbits weighted 3 ± 0.3 kg and were older than 14 weeks at the time of the surgery. About 50 % of the rabbits used were male and 50 % female. 6 Rabbits were used in the tracking study, 6 rabbits were used to optimize the transfection protocol, 6 rabbits were used as BMAC donors for ex-vivo studies and the remaining rabbits were used to assess the biological activity of TGF-β1 mRNA. *In vivo* transfection was optimized first in Sprague-Dawley male rats weighing approximately 350 g. For the pilot we used 6 rats and we delivered mRNA complexes generated with polymeric or with lipidic transfecting agents with or without FMCM. The firefly luciferase (FLUC)-encoding mRNA complexes were injected subcutaneously. More details about bioluminescence analysis are provided in the "luciferase imaging" paragraph below.

2.2.2. In vivo bone marrow collection

We collected bone marrow from the iliac crest of the rabbits. For the surgery, we administered Midazolam (0.5mg/kgIM) and Ketamine (10 mg/kg IM) as sedatives, and Buprenorphine (0.03 mg/kg IM) as a pain medication. The rabbits were then placed in an anesthesia chamber until anesthetized, then intubated and maintained on Isoflurane (0–4% in 100 % O2). A dose of Ceftiofur (40 mg/kg SQ), a broad-spectrum antibiotic, was administered at this time. After the pre-operative procedures described above had been performed, the surgical site on both legs was shaved and prepped with alternating scrubs of chlorohexidene and sterile saline prior to transfer to the surgical suite. In order to collect bone marrow, the rabbits were then placed in dorsal recumbency and surgically draped. A stab incision was made over the iliac crest and a bone biopsy needle used to collect bone marrow. The muscle layers subcutaneous tissues and skin were then closed using an absorbable suture (Polysorb™, Covidien). On average we were able to collect

between 0.5 and 1 mL of bone marrow aspirate from each rabbit.

2.2.3. Generation of BMAC

Bone marrow aspirates obtained from the rabbit iliac crest were collected in EDTA-coated tubes (Vacutainer, BD). The aspirates were promptly diluted with 4 mL of sterile PBS and concentrated by centrifugation at 2000 rpm for 5 min (Fig. 1A). The cell pellet was resuspended in 2 mL of PBS and mixed with 4 mL of red blood cell lysis buffer and incubated at room temperature for 10 min. The cell suspension (BMAC) was washed in PBS twice and resuspended in 200 μL IMDM.

2.2.4. Bone marrow clot formation with mRNA/FMCM complexes

We transferred 100 μL of the BMAC solution in a 96-well plate and mixed with mRNA-complexes loaded on FMCM as described above (Fig. 1A and B). In order to induce clot formation we used autologous peripheral blood. Approximately 400 μL of peripheral blood was drawn from the ear vein of the rabbits and promptly mixed with the BMAC-mRNA in the 96-well plate using approximately an equal volume of BMAC solution and peripheral blood. The clots were allowed to stabilize for 5 min at room temperature before use for the *in vivo* osteochondral defect studies.

2.2.5. In vivo rabbit osteochondral defect model

In order to create a bilateral osteochondral defect, the rabbits were then placed in a recumbent position, and the new surgical sites were sterilely prepped as described above and surgically draped. A 2-cm medial skin incision was made in one randomly selected medial femoral condyle to expose the bone. An osteochondral defect with a diameter of 2.7 mm and a depth of 3 mm was created on the medial condyle using a drill bit.

2.2.6. In vivo tracking of BMAC clots

To monitor the localization of BMAC clots within the osteochondral defect over time, we harnessed MCMs' protein-binding ability to load luciferase. We incubated 1 mg of MCM with 100 μg of Luciferase (Biosynth, L-8090) at room temperature for 1 h. After removing unbound luciferase through centrifugation, we resuspended the MCM in 50 μL of Optimem. Subsequently, we mixed the MCM with BMAC and obtained a clot by adding peripheral blood from the rabbit's ear vein and incubating for 5 min at room temperature. The rabbits were euthanized after 1 and 14 days and the legs containing the defects were collected and imaged immediately using an In Vivo Imaging System (IVIS) to monitor bioluminescence as described below (Supplementary Fig. S1).

2.2.7. Luciferase imaging

Luciferase imaging was used for: tracking BMAC clots and for the optimization of mRNA delivery subcutaneously in rats and for transfection optimization within osteochondral defects in rabbits. The animals or tissues were imaged for bioluminescence using an In Vivo Imaging System (IVIS) (PerkinElmer). For the subcutaneous pilot study in rats, the animals were anesthetized in an induction chamber delivering 4 L O_2/min with 4 % isoflurane and then placed in the *in vivo* imaging chamber equipped with a nose cone delivering maintenance isoflurane (0.8 % isoflurane, O_2 delivery rate of 2–3 L/min). The substrate solution (containing 100 mM of ATP and 0.5 mM D-luciferin; Biosynth, L-8220) was injected in the proximity of the area of interest and we started the imaging process 1 min post injection (Supplementary Fig. S2). Regarding the tracking study and the optimization of transfection in osteochondral defects, the rabbits were euthanized after 1 and 14 days and the legs containing the defects were imaged using IVIS. The substrate solution was injected directly inside the defect, rupturing the clot to ensure the diffusion of the substrate within the defect. The tissues were imaged immediately post-injection.

2.2.8. Assessment of the biological effect of TGF-β1-mRNA in a rabbit model of osteochondral defect

Each rabbit underwent bilateral surgery, with one leg designated for an empty defect control and the opposite leg for the treatment application. We included a separate empty defect control group to mitigate potential systemic effects on the control group's performance. The study used 6 rabbits per group and comprised the following groups: empty defect control, clot alone, BMAC clot, BMAC clots-MCM, BMAC clot-FMCM, and BMAC clot-FMCM-TGF-β1-mRNA. The processed bone marrow clot was placed in the defect, and absorbable sutures were used to close the joint capsule, fasciae, and skin incision. The contralateral medial condyle underwent the same procedure but did not receive any treatment, serving as the control. The side that received the treatment was selected randomly at each surgery. Rabbits were euthanized at 9 weeks for histology/immunohistochemistry analyses and at 21 days for quantitative RT-PCR and ELISA. FMCM was the delivery system of choice throughout the *in vivo* studies, since we saw greater production of the mRNA-encoded transgene when the delivery had been performed with FMCM when compared to the MCM. Therefore, we focused our attention on this group for the subsequent experiments and present data only from the FMCM group and from its relative control in the main results.

2.2.9. Histological assessment of cartilage regeneration

Immunohistochemistry (IHC) was performed to detect type I and type II collagen. Upon collection, the tissues were fixed in 10 % formalin, trimmed and decalcified before being embedded in paraffin. Paraffin-embedded samples were cut at 5 μm thickness and mounted on charged microscope slides. Samples were deparaffinized in citrisolv and rehydrated in a series of graded ethanol solutions. Enzymatic antigen retrieval was performed using 0.1 % pepsin in 0.01N HCl. Samples were then exposed to 3 % hydrogen peroxide to eliminate endogenous peroxidase activity, blocked using normal serum (Vector Laboratories, Burlingame, CA), and incubated with mouse primary antibodies to detect type I collagen (5 μg/ml, ab6308, Abcam, Cambridge, MA) and type II collagen (2 μg/ml, II-II6B, Developmental Studies Hybridoma Bank). After primary antibody application, sections were exposed to biotinylated anti-mouse secondary antibody, then administered avidin-biotin horseradish peroxidase complex using the Vectastain Elite ABC peroxidase kit (PK-6102, Vector Laboratories). The bound antibody complex was visualized using diaminobenzidine (DAB; Innovex Biosciences). Stained sections were dehydrated with a series of graded ethanol solutions, cleared, and cover-slipped. Negative controls omitting the primary antibody were included with each experiment. Samples were also stained for H&E and Safranin O to measure the extent of defect and cartilage healing, respectively. Stained samples were imaged using an Aperio Digital Pathology Slide Scanner. The images relative to H&E stain, Safranin-O stain, and collagens IHC were used to assess the O'Driscoll score. The score was determined by grading the following aspects of cartilage healing: deposition of GAGs near the surface and throughout the defect, surface irregularities, surface integrity, cartilage thickness, bonding to adjacent tissues, cellular phenotype (shape, size and density), presence of cellular clusters, reconstitution of subchondral bone, bonding of repaired cartilage to subchondral bone. The grading was performed by 4 independent users and the grades were averaged prior to be used to calculate the final score.

2.2.10. Image analysis

Open source softwares such as ImageJ and Qupath were used for imaging analysis. The difference in color between treatment and controls was assessed by using ImageJ. The area of interest was selected and the pixels were quantified using the "analyze" and "histogram" function of ImageJ. The quantification of stain intensity from IHC or histological images was obtained using ImageJ-Fiji. The region of interest relative to the stain to be quantified was selected using the color deconvolution feature of ImageJ. The mean density of the stain was obtained by

selecting analyze and then measure. The optical density was then calculated by using the following formula: LOG(255/mean intensity). The area of the stained regions were calculated using the measure function of ImageJ under the analyze tab. Cell density and cell shape was determined using Qupath to open images of H&E-stained slides. The region of interest was selected and the function "cell detection" was used to detect and quantify cell parameters such as cell number and circularity. The cell density of the analyzed areas was calculated by using the following formula: cell number/area. Qupath was used also to take surface measurements such as length and width. The fibrillation index was calculated by dividing the length of the fibrillated area (L) by the width (W) of the measured area as suggested in literature [26].

2.3. Quantitative RT-PCR

After euthanasia, the area of the osteochondral defects was separated from the surrounding tissues using a bone saw and immersed in mRNA/DNA shield solution (Zymo Research) and frozen at −80 °C until use. The clot tissue implanted within the defect was collected using a spatula and the defect was rinsed using mRNA/DNA shield solution to collect as much tissue as possible. The clots were collected in a 1.5 mL tube containing stainless steel beads and processed in a tissue homogenizer (Bullet Blender Storm24 - Nextadvance). Total RNA was extracted from cells using the Zymo Quick-RNA MicroPrep kit (Zymo Research) following the manufacturer directions. To synthesize cDNA, 1 μg of total RNA was used to synthesize cDNA using the High-Capacity cDNA Reverse Transcription kit (Applied Biosystems). Quantitative RT–PCR was performed using iQ SYBR Green Premix (Bio–Rad) with primers pairs specific for the following genes: ABI family member 3 binding protein (Abi3bp), thrombospondin-4 (Thbs4), SRY-box transcription factor-9 (SOX9), proteoglycan-4 (PRG4), Collagen II, SIX homeobox-1 (SIX1), Alkaline phosphatase-1 (ALPI), Collagen X, Collagen I, transforming growth factor beta-1 (TGF-β1).

2.4. Statistics

The results are presented as mean ± SD. The statistical comparisons were made using paired Student's *t*-test or one-way ANOVA with Tukey's post hoc test, and the statistical significance was determined to be $p < 0.05$. The statistical analysis was performed using GraphPad Prism version 7. The correlation study was done using Python. The Pearson's coefficient was calculated and the following libraries where used to generate a heatmap representing correlations: pandas, seaborn, and matplotlib.

3. Results

3.1. BMAC clots were localized in vivo

Tracking studies *in vivo* revealed that BMAC clots were maintained in osteochondral defects for at least 2 weeks post-surgery (Fig. 1C). This is in line with what observed in other studies conducted in different animal models where clots were observed for up to 15 days *in vivo* [27]. The versatility of MCMs allowed for tracking the clot *in vivo*. In fact, clots without MCMs failed to retain reporter FLUC and could not be detected even after just one day post-surgery. The use of MCMs not only prevented leakage of FLUC outside the clots, but also maintained prolonged FLUC activity to 2 weeks (Fig. 1C), even though FLUC usually has a half-life of just 4 h *in vivo* [28]. This ability of MCMs to maintain protein activity and prolong half-life has been detailed in our previous studies [23,29].

3.2. Delivery of therapeutic mRNA to BMAC clots increased TGF-β1 production

The efficacy of mRNA delivery to BMAC cells was influenced by the MCM properties, the presence of anticoagulants (Fig. 2A), and the type of mRNA complexing agent used (Fig. 2B). The study utilized a custom mRNA sequence that effectively encoded human TGF-β1 (Fig. 2C). Upon delivery to BMAC clots *ex-vivo*, there was a significant increase in TGF-β1 secretion from the clots (Fig. 2D). Higher *in vitro* transfection of BMAC occurred when cells were cultured in IMDM media (Supplementary Fig. S3), and when TGF-β1-mRNA complexes were delivered using fluoride-doped MCMs (FMCMs) (Supplementary Fig. S4A). Moreover, the anticoagulants used during BMAC processing also affected mRNA transfection. Heparin had a negative impact on transfection compared to standard delivery of mRNA complexes via FMCMs, while EDTA was associated with a significant increase in transfection when mRNA complexes were delivered using FMCMs (Fig. 2A).

The use of FMCM to deliver mRNA complexes also influenced transfection *in vivo*. Subcutaneous injections of lipidic mRNA complexes bound to FMCM transfected cells in proximity of the injection site (Supplementary Fig. S2). On the other hand, soluble delivery (without FMCM) led to the diffusion of mRNA complexes out of the injection area (Supplementary Fig. S2). This localizing effect of mRNA delivery via FMCM has been highlighted also in a previous study [30]. The targeted environment and mRNA delivery method also influenced transfection *in vivo*. mRNA condensed with the lipidic transfecting agent MessengerMax produced transfection when injected subcutaneously but did not effectively transfect cells in osteochondral defects (Fig. 2B). In contrast, mRNA complexed with the polymeric transfecting agent TransIT showed higher transfection than lipidic transfecting agents in osteochondral defects (Fig. 2B). When BMAC clots were transfected with TGF-β1-mRNA we measured over a 3000-fold increase in TGF-β1-mRNA presence within the cells after being implanted for 2 days (Supplementary Fig. S5). In addition, mRNA was only quantifiable by RT-PCR after the dissociation of the mRNA complexes inside the cells, and intact mRNA complexes were not quantifiable by RT-PCR (Supplementary Fig. S6). Therefore, RT-PCR analysis confirmed that mRNA was successfully delivered to the cells within the osteochondral defects (Supplementary Fig. S5).

3.3. mRNA-activated clots implanted in vivo increased the expression of chondrocyte markers and improved macroscopic appearance of healing osteochondral defects

BMAC clots treated with TGF-β1-mRNA complexed with polymeric transfecting agent and delivered via FMCM showed a significant improvement in macroscopic appearance (Fig. 3A and B). The defects that received BMAC had significantly higher cell density than empty defect controls (Fig. 3C) and also higher circularity (Fig. 3D). TGF-β1-mRNA delivery to BMAC clots induced a significant increase in the early expression of several articular chondrocyte markers within the osteochondral defects after 2 days post-surgery (Fig. 4A). The articular chondrocyte markers that were upregulated were: Abi3bp, Thbs4, SOX9 and PRG4 while only one marker of growth plate chondrocytes was upregulated: ALPI (Fig. 4A). Moreover, the TGF-β1-mRNA treated BMAC conditions showed significant improvement in macroscopic appearance of the defects at 9 weeks post-surgery relative to empty defect controls (Fig. 3A). The empty defects and defects that received only BMAC clots without mRNA were white in appearance, a hallmark of fibrotic tissues [31]. In contrast, the mRNA-treated defects had a less prominent color difference relative to the surrounding tissues and without clear delimitation between repaired and native cartilage (Fig. 3A).

O'Driscoll scoring to assess the quality of healing among the different experimental groups showed substantial variability and no statistically significant differences in the treatment groups (Fig. 4B and C). Further analysis of the O'Driscoll score revealed that mRNA-treated defects showed improved GAG deposition but low surface integrity (Fig. 4C). However, quantification of the fibrillation index by imaging analysis showed that the differences in surface integrity between mRNA-treated

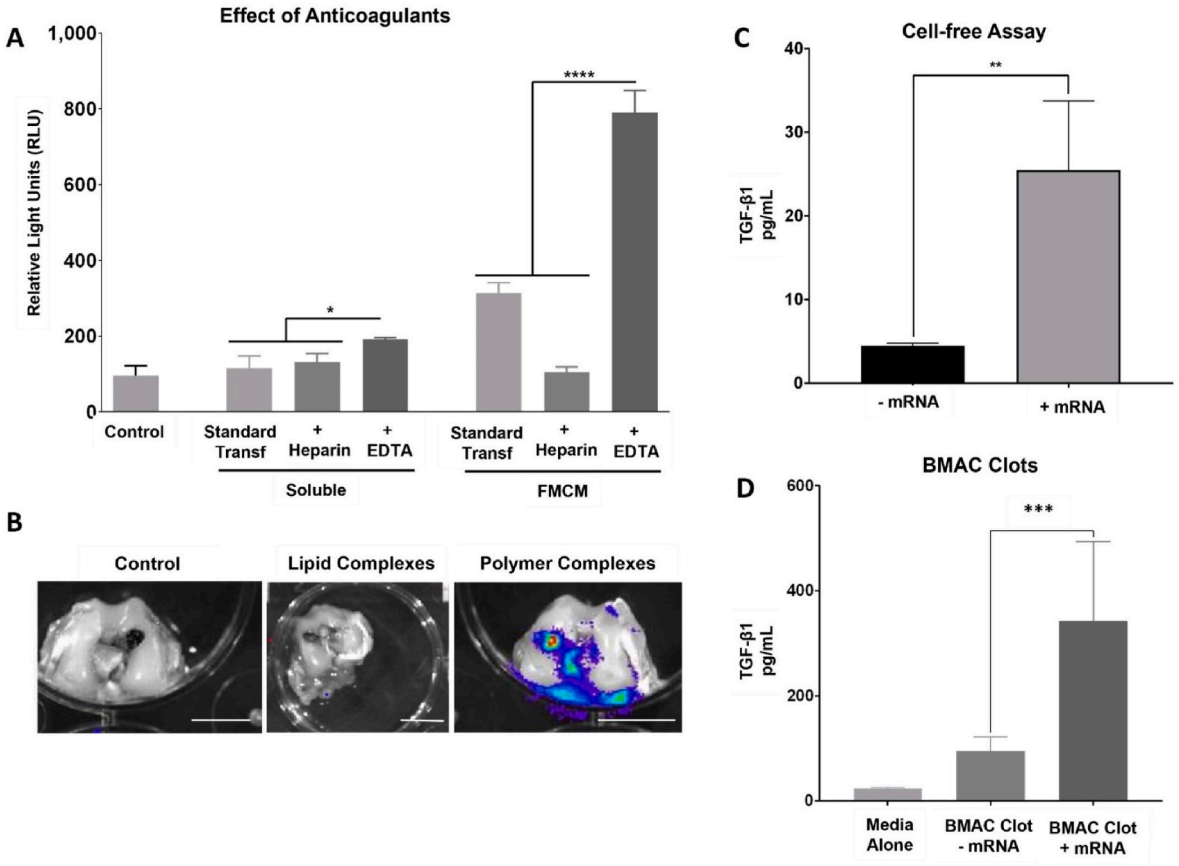

Fig. 2. Delivery of therapeutic mRNA to BMAC clots increases TGF-b1 production. (**A**) Comparison of the effects of anticoagulants on *in vitro* transfection of rabbit BMAC using mRNA delivered via FMCM or in soluble form. (*) represents statistically significant differences using one-way analysis of variance (ANOVA) followed by Tukey's multiple comparisons test, n = 4, *p < 0.05 and ****p < 0.0001. (**B**) Representative (IVIS) images of osteochondral defects explants that received BMAC clots bearing FLUC-mRNA complexes obtained with lipidic or polymeric complexing agents. All the mRNA complexes were delivered using FMCM and the tissue was harvested 2 days post-transfection. Scalebar = 5 mm. (**C**) Total amount of TGF-β1 produced from custom mRNA sequences. The mRNA was translated by a cell-free rabbit reticulocyte lysate system and the TGF-β1 quantified by ELISA. (*) represents statistically significant differences using one-way analysis of variance (ANOVA) followed by Tukey's multiple comparisons test, n = 4, *p < 0.05 and **p < 0.01. (**D**) Total TGF-β1 secreted by BMAC clots with or without TGF-β1-mRNA and cultured *ex-vivo* for 2 days. Asterisk represents statistically significant differences using paired Student's *t*-test (n = 4), ***p < 0.001.

defects and controls were not statistically significant (Fig. 4D).

3.4. mRNA-activated clots significantly decreased fibrocartilage formation in vivo

Treatment of BMAC clots with TGF-β1-mRNA resulted in a significant reduction in collagen I deposition compared to controls, as observed after 21 days and maintained for 9 weeks (Fig. 5). Moreover, the treatment elicited an increase in collagen II deposition after 9 weeks (Fig. 5). ELISA analysis confirmed that TGF-β1-mRNA delivery caused a significant decrease in the type I/type II collagen ratio from 0.825 ± 0.022 to 0.565 ± 0.010 (Fig. 5). This shift in collagen ratios was primarily driven by a substantial decrease in collagen I deposition, as evidenced by the reduced amount of collagen I in mRNA-treated defects (Fig. 5). Furthermore, cell shape analysis revealed significant differences between mRNA-treated defects and empty defect controls (Fig. 3D). Cells within the empty defect controls exhibited an elongated and fibroblast-like shape, while cells in mRNA-treated defects displayed a more circular shape, resembling the characteristic morphology of chondrocytes. Additionally, a correlation analysis between collagen deposition revealed that in empty defect controls there was a direct correlation between the deposition of type I and type II collagen (Supplementary Fig. S12). However, in mRNA-treated defects, the deposition of type I and type II collagen showed an inverse correlation, suggesting that increased type II collagen coincided with reduced type I collagen production (Supplementary Fig. S12).

3.5. GAG deposition area was increased in mRNA-treated defects compared to empty defects

GAG deposition in mRNA-treated defects covered 42 ± 17.9 % of the area, significantly more than the 19 ± 12.5 % observed in empty defect controls (Fig. 6). The mRNA-treated defects also obtained the highest GAG deposition score according to the O'Driscoll score (Fig. 4B). Notably, GAGs deposition primarily occurred in the middle zone rather than the surface zone across all groups (Fig. 6).

4. Discussion

The delivery of TGF-β1-mRNA to autologous BMAC clots decreased collagen I deposition, increased stain intensity for type II collagen (Fig. 5) and improved macroscopic appearance (Fig. 3) suggesting lower fibrocartilage formation. The delivery of TGF-β1 mRNA to BMAC clots markedly increased the secretion of TGF-β1 compared to that in untreated BMAC clots (Fig. 2D). Despite the presumably transient nature of the mRNA expression, we observed longer-term biological effects. Notably, BMAC clots treated with TGF-β1 mRNA maintained a higher ratio of collagen II to collagen I throughout the cartilage repair process (Fig. 5). This suggests that mRNA treatment influences the collagen composition of repaired tissue. TGF-β1 mRNA delivery significantly

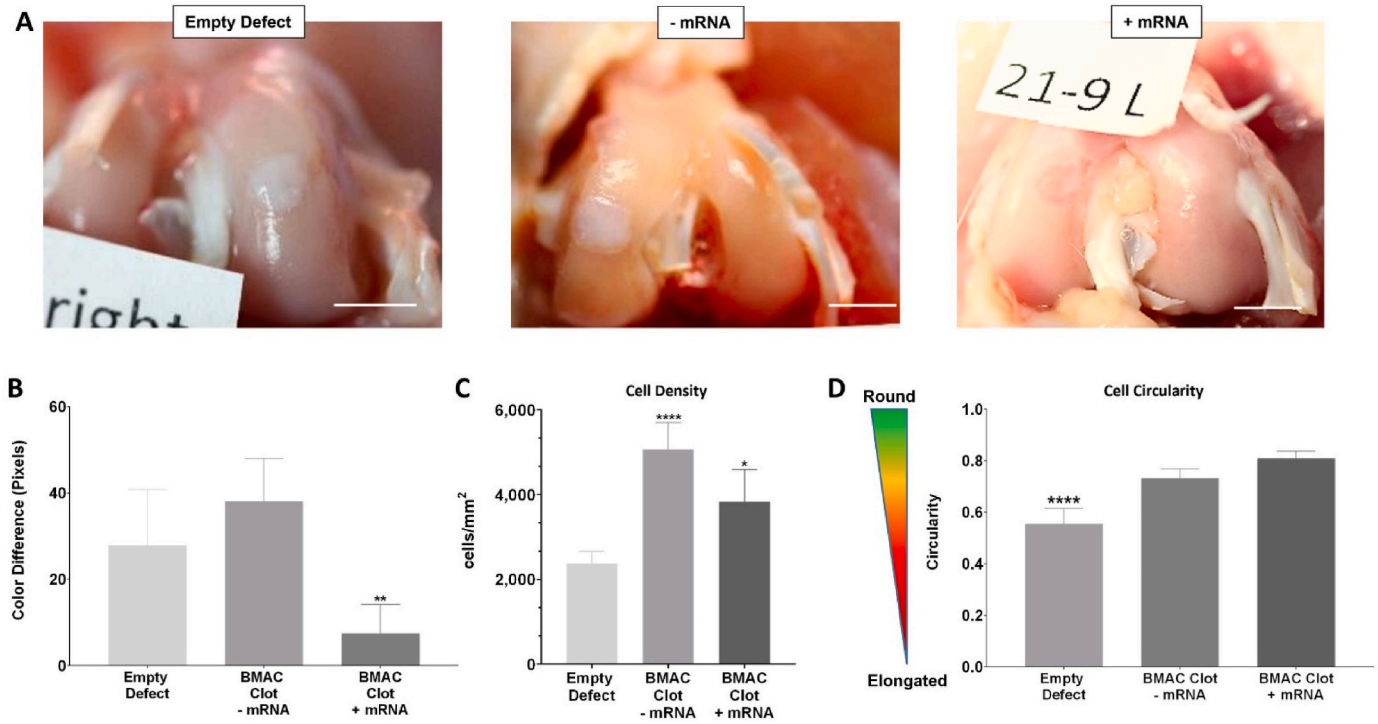

Fig. 3. mRNA-activated clots implanted *in vivo* improve the macroscopic appearance of osteochondral defects. (**A**) Osteochondral defects collected 9 weeks post-surgery. The empty defect control and the BMAC clot without mRNA have a white appearance, indicative of fibrocartilage. On the other hand, the BMAC clot treated with TGF-β1 mRNA has better macroscopic appearance. Scalebar = 5 mm. (**B**) Quantification of color difference between defect area and the surrounding tissue, the mRNA-treated defects show significantly lower color difference with the adjacent tissue compared to the control groups. (*) represents statistically significant differences using one-way analysis of variance (ANOVA) followed by Tukey's multiple comparisons test, n = 4, **p < 0.01. (**C**) Quantification of cell density obtained from the analysis of H&E-stained sections reveal that the delivery of BMAC through clots increased significantly the cellular density of the defects compared to empty controls. (*) represents statistically significant differences using one-way analysis of variance (ANOVA) followed by Tukey's multiple comparisons test, n = 4, *p < 0.05 and ***p < 0.001. (**D**) Comparison of cell circularity within the defects. The analysis was conducted on H&E sections and the cell shape assessed using the software QuPath. The analysis revealed that cells in empty defect controls were significantly more elongated compared to cells within BMAC clots treated with TGF-β1-mRNA. (*) represents statistically significant differences using paired Student's *t*-test (n = 4, ***p < 0.001.

reduced collagen I production in BMAC clots after 21 days (Fig. 5A). Over time, the observed effect had a persistent impact. This resulted in a significant decrease in collagen I deposition after 9 weeks (Fig. 5D). At the macroscopic level, the control defects exhibited a white appearance and distinct color differences from the surrounding tissue (Fig. 3A), suggesting fibrocartilage formation [32]. In contrast, defects treated with TGF-β1 mRNA did not exhibit clear boundaries from neighboring tissues (Fig. 3A) and displayed reduced color differences compared to healthy adjacent tissues (Fig. 3B). The untreated defects and BMAC clot controls showed signs of fibrocartilage formation, characterized by their white appearance (Fig. 3A), elongated cells (Fig. 3D), and an evident increase in collagen I deposition (Fig. 5A). However, in BMAC clots treated with TGF-β1 mRNA, there was a significant reduction in fibrocartilage formation. This was demonstrated by a considerable decrease in collagen I deposition (Fig. 5A), cells exhibiting chondrocyte-like morphology with higher shape factors (Fig. 3D), and an improved overall appearance at the macroscopic level (Fig. 3A).

Previous investigations have consistently demonstrated the prevalence of fibrocartilage formation during the healing process of rabbit osteochondral defects [33]. While fibrocartilage has been associated with favorable short-term outcomes for patients, clinical studies have revealed a general failure of fibrocartilage within a decade [16]. This occurs because fibrocartilage lacks the biochemical and viscoelastic properties that characterize hyaline cartilage [16].

Autologous tissues offer a promising avenue for tissue engineering, providing potential benefits for healing outcomes. Previous studies have demonstrated the effectiveness of autologous tissues, including platelet-rich plasma (PRP) [34], bone marrow aspirate concentrate (BMAC) [6], and bone marrow aspirate (BMA) [18], in improving tissue repair. Since there are no effective pharmacological interventions for cartilage regeneration, surgical intervention becomes paramount for individuals with osteoarthritis (OA) [35]. One such surgical procedure is microfracture surgery, which leverages the regenerative capacity of surrounding tissues to heal damaged cartilage. Following this surgery, a bone marrow clot forms and undergoes remodeling to develop into a fibrocartilage plug enriched with type I collagen [16]. However, these benefits are temporary as the fibrocartilage plug possesses inferior mechanical properties compared to healthy cartilage [16].

Because of the limitations of microfractures, alternative techniques for harnessing autologous tissues have been explored with limited success. For example, the use of PRP has demonstrated mixed outcomes, making its evaluation challenging [36]. In contrast, clinical outcomes associated with BMA utilization were found to be influenced by factors such as the concentration of human mesenchymal stem cells (hMSCs) in the BMA, and the donor's age [37]. BMA delivery outcomes vary significantly, making it less effective in elderly patients with lower cell counts. One solution could involve supplementation of BMA with *in vitro*-expanded hMSCs [38]. However, the clinical translation of such an approach would face additional regulatory hurdles and likely encounter limitations commonly associated with the *in vitro* expansion of hMSCs [8]. Instead, the use of BMAC demonstrated favorable outcomes, including enhanced histological scoring and increased deposition of GAGs in relevant translational *in vivo* models [6,19]. Moreover, the beneficial effects of BMAC were evident in the non-supplemented BMAC control groups in this study. The inclusion of BMAC in all clots, including the controls, led to a significant increase in the cellular density within

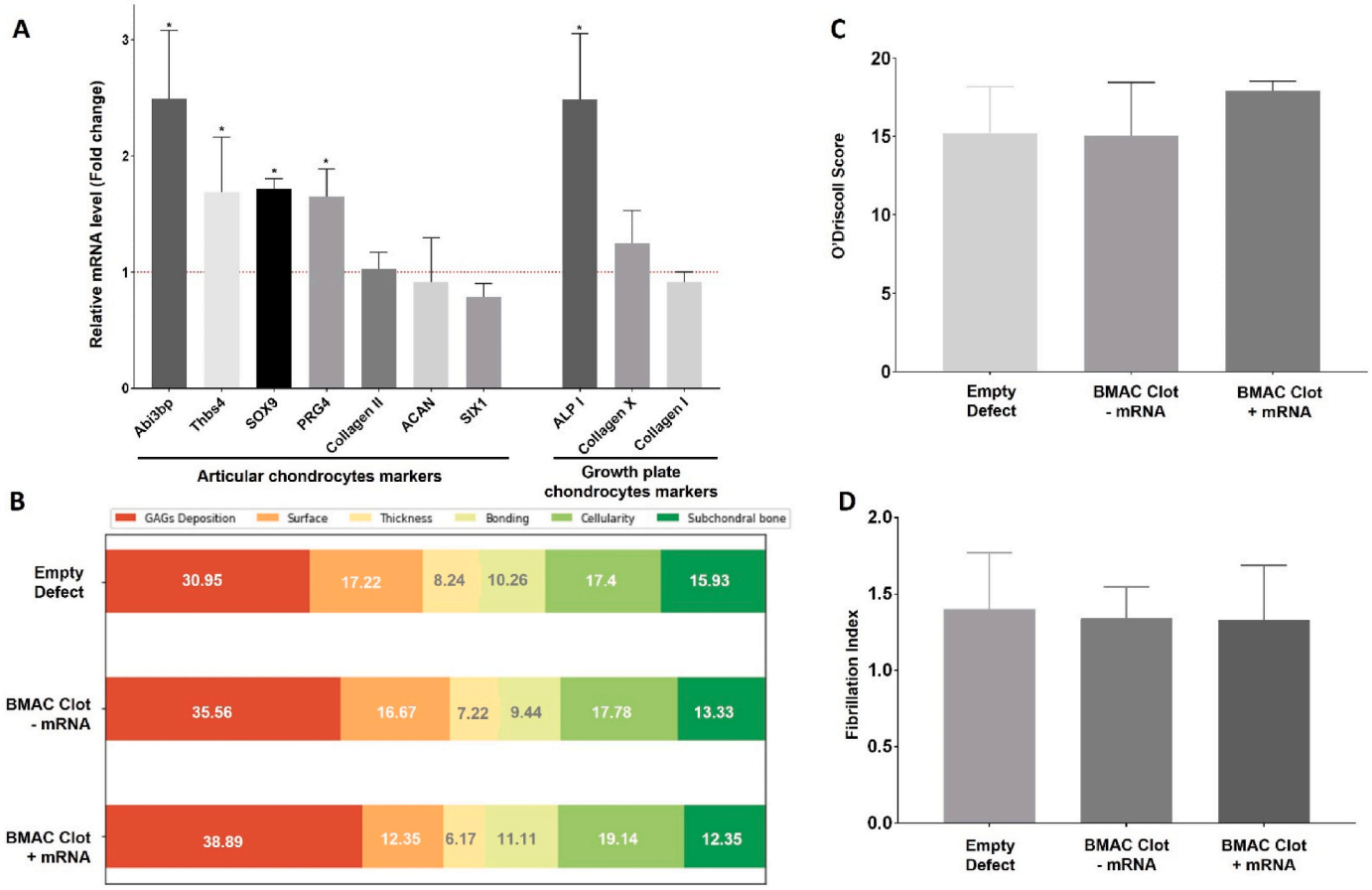

Fig. 4. mRNA-activated clots implanted *in vivo* increase the expression of chondrocyte markers within osteochondral defects. (**A**) RT-PCR analysis of osteochondral defects 2 days post-surgery. Defects treated with BMAC clots and TGF-β1-mRNA were compared to BMAC clots without TGF-β1-mRNA, the results indicate a significant increase in the expression of some articular chondrocytes markers in the mRNA-treated group. (*) represents statistically significant differences using paired Student's *t*-test ($n = 4$), $p < 0.05$. (**B**) Breakdown of the O'Driscoll score reveal that GAGs deposition was the major contributor to the score of the mRNA-treated clots. (**C**) The O'Driscoll score of the treatment groups was obtained from the histological analysis of Safranin-o and H&E-stained sections. (**D**) The fibrillation index was obtained by dividing the length of the fibrillated surface by the width of the fibrillated area. The analysis showed that there weren't significant differences between the treatments.

the defects (Fig. 3C). Furthermore, the morphological characteristics of the cells within these defects closely resembled those of chondrocytes (Fig. 3D), highlighting the regenerative potential of BMAC.

The current study takes a novel approach by introducing therapeutic mRNA into BMAC clots to activate a specific healing mechanism. Although expression of the mRNA transgene was likely short-lived, the therapeutic effect was observed at the 9-week endpoint. There are several potential reasons for this observation. First, a significant increase in the expression of articular chondrocyte markers was detected in BMAC clots treated with TGFβ1-mRNA as early as 2 days post-treatment (Fig. 4A). The administration of TGFβ1-mRNA resulted in the upregulation of several articular chondrocyte markers, including Abi3bp, Thbs4, Sox9, and Prg4. However, among the growth plate chondrocyte markers, only AlpI was upregulated (Fig. 4A). These markers play pivotal roles in maintaining cartilage homeostasis. For instance, Prg4, a synovial joint glycoprotein, alleviates shear stress at the cartilage surface and mitigates inflammation within the tissue [39]. Sox9, a key transcription factor, orchestrates cartilage homeostasis by inducing the expression of essential extracellular matrix (ECM) proteins such as collagen II and aggrecan [40]. Furthermore, thbs4 expression correlates with cartilage thickness *in vivo* [41]. The early upregulation of these genes may have contributed to the observed reduction in fibrocartilage formation at the 9-week post-surgery time point (Fig. 5). A second possible explanation for the sustained biological impact of mRNA delivery is the use of FMCM. Prior *in vivo* research has demonstrated that FMCM can stabilize biologics [42], and when used to deliver mRNA complexes, they can sequester and stabilize the protein produced by the mRNA, thereby amplifying the biological activity and therapeutic effectiveness for a prolonged period [23]. A third possible explanation for the prolonged biological activity observed in the treatment group is that the early expression of articular chondrocyte markers (Fig. 4A) and the significant increase in the area of GAGs deposition (Fig. 6) may have created an environment that prevented collagen I deposition. The biological activity of TGF-β1 may have been influenced by GAGs deposition. Previous studies have shown that the presence of aggrecan, GAGs and hyaluronic acid/CD44 complexes can enhance the anabolic effects of TGF-β1 [24,43,44]. The anabolic or catabolic effects of TGF-β1 are context-dependent, and the conventional delivery of TGF-β1 protein using supra-physiological doses may lead to an increase in catabolic effects [24]. In this study, TGF-β1 was produced directly within defects and at concentrations within the physiological range. mRNA treatment induced a wider distribution of GAGs within the defects, which may support the anabolic effects of TGF-β1.

Although combination of TGF-β1-mRNA and BMAC clots substantially decreased fibrocartilage formation, it is important to note that the outcome could be improved further. For example, more abundant GAGs deposition and higher surface integrity would be desirable. This highlights the limitations of using a single growth factor as a target and emphasizes the need for approaches that enable the delivery of multiple therapeutic mRNAs to promote regenerative healing. Osteochondral

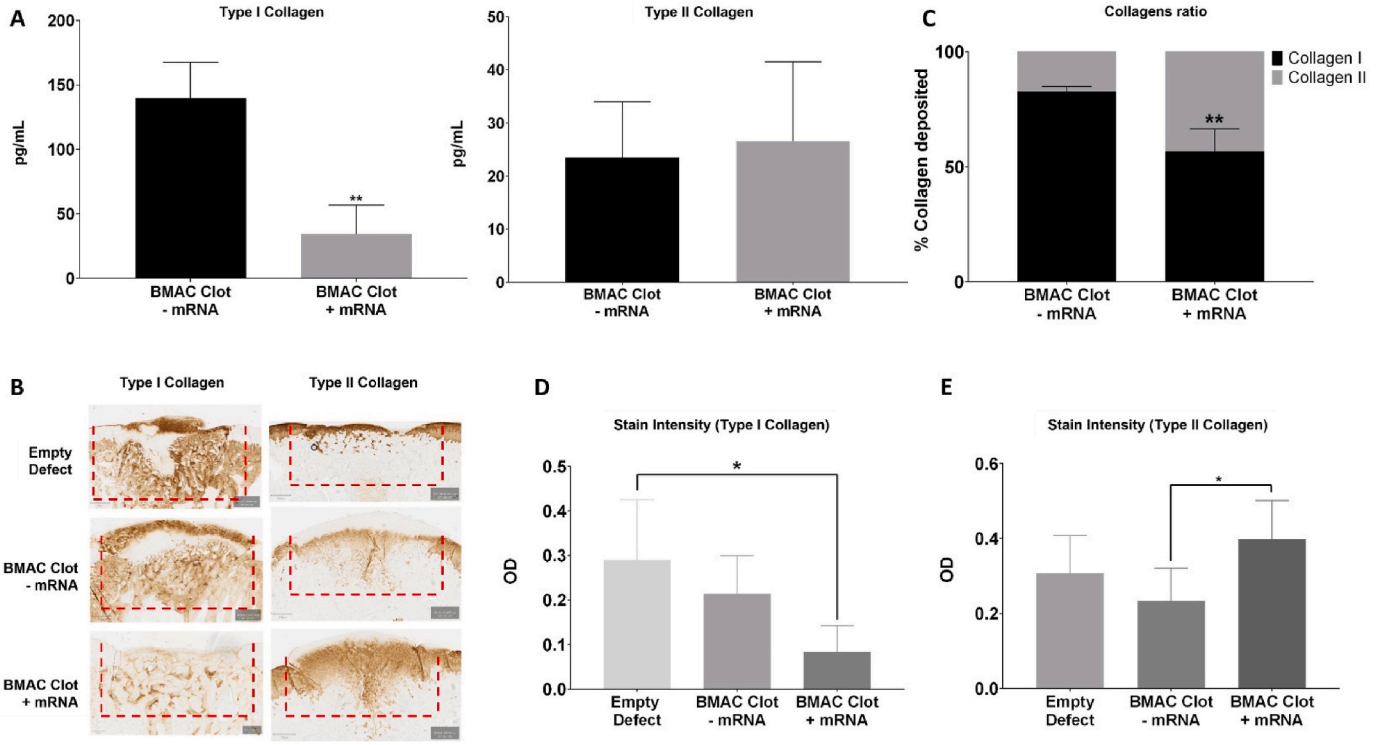

Fig. 5. Delivery of mRNA-activated clots significantly decreases the formation of fibrotic tissue *in vivo*. (**A**) Amount of type I collagen and type II collagen deposited in the defects 21 days post-surgery and quantified via ELISA. (*) represents statistically significant differences using one-way analysis of variance (ANOVA) followed by Tukey's multiple comparisons test, n = 4, **p < 0.01 (**B**) Anti-collagen staining (left: Anti-collagen I; right: Anti-collagen II) of osteochondral defects 9 weeks post-surgery. Scalebar = 400 μm. (**C**) The ratio of collagen I to collagen II in osteochondral defects 21 days post-surgery was determined by ELISA. BMAC clots without TGF-β1-mRNA had 82.5 ± 2.2 % of collagen I and the BMAC clots treated with TGF-β1-mRNA showed a reduction to 56.5 ± 10 % of collagen I, the difference between treatments was significant. (*) represents statistically significant differences using paired Student's *t*-test (n = 4, **p < 0.01. (**D**) The mRNA-treated BMAC clots showed significantly lower stain intensity for collagen I compared to the empty defects controls. (*) represents statistically significant differences using one-way analysis of variance (ANOVA) followed by Tukey's multiple comparisons test, n = 4, *p < 0.05. (**E**) The mRNA-treated BMAC clots showed significantly higher stain intensity for collagen II compared to BMAC clots without TGF-β1-mRNA. (*) represents statistically significant differences using one-way analysis of variance (ANOVA) followed by Tukey's multiple comparisons test, n = 4, *p < 0.05.

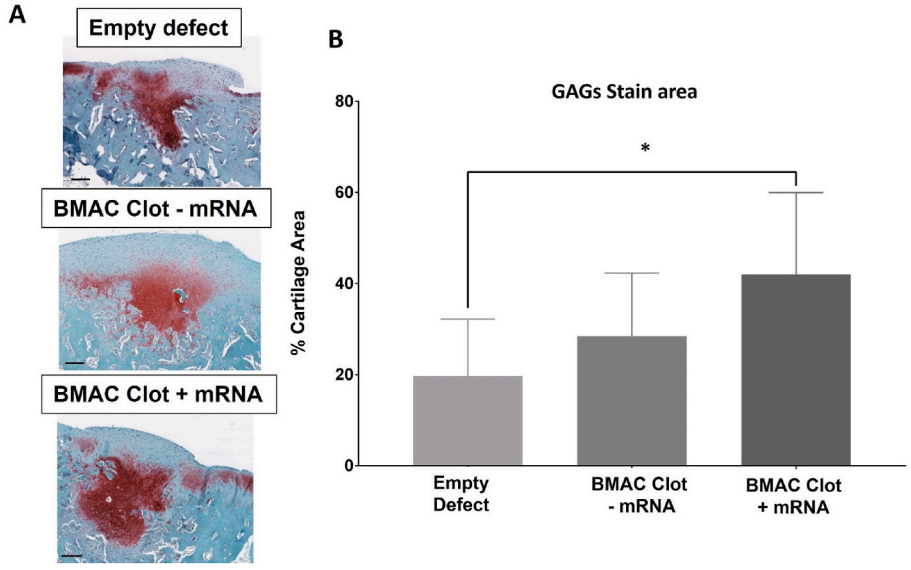

Fig. 6. Wider GAGs deposition area in mRNA-treated defects compared to empty defects. (**A**) Safranin-o stained sections of osteochondral defects 9 weeks post-surgery. Collagens are stained blue while GAGs are stained red. Scalebar = 250 μm. (**B**) Quantification of GAGs staining area shows that the BMAC clots treated with TGF-β1-mRNA have significantly higher stain area than empty defects controls. (*) represents statistically significant differences using one-way analysis of variance (ANOVA) followed by Tukey's multiple comparisons test, n = 4, *p < 0.05.

defect repair is a complex process involving multiple layers. The present study focused on the articular cartilage layer because it is the primary site of cartilage degeneration in OA and the most challenging layer for repair. Although our findings are promising for cartilage repair, further investigations are necessary to elucidate the underlying mechanisms of repair and to optimize the delivery strategy for clinical translation.

The animal model used in this study also has limitations. Rabbits remarkable healing capabilities to the extent that even empty defects demonstrate some level of cartilage repair at 12 weeks [45]. The duration of this study was intentionally limited to nine weeks to facilitate the examination of the early stages of cartilage repair. Future studies can extend this approach to larger animal models over a longer duration to establish the therapeutic potential. Moreover, since the inception of this study, new formulations of lipid nanoparticles have been developed for mRNA delivery, which may enable the delivery of larger amounts of mRNA with higher transfection efficiency and low toxicity [46]. Transfection can also be improved by further optimizing the mRNA delivery environment. We showed that the surrounding environmental conditions significantly influence BMAC transfection, with the choice of anticoagulant playing a crucial role. Heparin reduced transfection efficacy, whereas EDTA enhanced it (Fig. 2A). Although previous *in vitro* studies favored regular MCMs for lipid-complexed mRNA delivery to BMAC [47], FMCMs showed better performance for polymer-complexed mRNA (Supplementary Fig. S4). The unique nanoscale topography of FMCMs [30] and the impact of MCM-released ions on endocytosis [47] may contribute to these differences. Additionally, FMCMs maintained transfection localized at the injection site over time (Supplementary Fig. S2), which is crucial for avoiding the potentially adverse effects of TGF-β1 leakage. Furthermore, the use of bone marrow and blood clots in osteochondral defects has been shown to minimize the leakage of biologics to surrounding tissues [38].

5. Conclusions

This study demonstrated the potential of therapeutic mRNA delivery to obtain long-term effects on cartilage repair. By functionalizing autologous BMAC clots with TGF-β1-mRNA and utilizing FMCMs as delivery vehicles, we obtained a reduction in fibrocartilage formation. This study demonstrated that even a single dose of transiently expressed therapeutic mRNA had a sustained effect on the regenerative potential of autologous BMAC. Future research may extend this approach to develop mRNA-based strategies to produce multiple therapeutic proteins, aiming to improve cartilage repair in larger animal models of osteochondral regeneration.

CRediT authorship contribution statement

Gianluca Fontana: Writing – review & editing, Writing – original draft, Visualization, Project administration, Methodology, Investigation, Formal analysis, Data curation, Conceptualization. **Brett Nemke:** Methodology, Conceptualization. **Yan Lu:** Methodology. **Connie Chamberlain:** Writing – review & editing, Data curation. **Jae-Sung Lee:** Writing – review & editing, Methodology. **Joshua A. Choe:** Writing – review & editing, Methodology. **Hongli Jiao:** Methodology. **Michael Nelson:** Methodology. **Margot Amitrano:** Methodology. **Wan-Ju Li:** Writing – review & editing, Conceptualization. **Mark Markel:** Supervision, Resources, Conceptualization. **William L. Murphy:** Writing – review & editing, Supervision, Investigation, Funding acquisition, Conceptualization.

Data availability

Data will be made available on request.

Ethics approval and consent to participate

All procedures involved in the animal study were approved by the University of Wisconsin-Madison Institutional Animal Care and Use Committee (approval number: V006006-R02).

Declaration of competing interest

The authors declare that they have no known competing financial interests or personal relationships that could have appeared to influence the work reported in this paper.

Acknowledgments

This study was funded by a generous philanthropic gift from the Shannon Family in support of the Musculoskeletal Regeneration Partnership. Joshua A. Choe was supported by the National Institute on Aging of the National Institutes of Health under Award Number F30AG077748 and the University of Wisconsin – Madison Medical Scientist Training Program: T32GM140935. The content is solely the responsibility of the authors and does not necessarily represent the official views of the National Institutes of Health.

Appendix A. Supplementary data

Supplementary data to this article can be found online at https://doi.org/10.1016/j.bioactmat.2024.11.033.

References

[1] T. Vos, et al., Global, regional, and national incidence, prevalence, and years lived with disability for 310 diseases and injuries, 1990–2015: a systematic analysis for the Global Burden of Disease Study 2015, Lancet 388 (2016) 1545–1602.
[2] E. Losina, et al., Lifetime risk and age at diagnosis of symptomatic knee osteoarthritis in the US, Arthritis Care Res. 65 (2013) 703–711.
[3] W.E. Van Spil, O. Kubassova, M. Boesen, A.C. Bay-Jensen, A. Mobasheri, Osteoarthritis phenotypes and novel therapeutic targets, Biochem. Pharmacol. 165 (2019) 41–48.
[4] A.K. Williamson, A.C. Chen, K. Masuda, E.J.-M.A. Thonar, R.L. Sah, Tensile mechanical properties of bovine articular cartilage: variations with growth and relationships to collagen network components, J. Orthop. Res. 21 (2003) 872–880.
[5] A.R. Armiento, M. Alini, M.J. Stoddart, Articular fibrocartilage - why does hyaline cartilage fail to repair? Adv. Drug Deliv. Rev. 146 (2019) 289–305.
[6] E.J. Cotter, K.C. Wang, A.B. Yanke, S. Chubinskaya, Bone marrow aspirate concentrate for cartilage defects of the knee: from bench to bedside evidence, Cartilage 9 (2018) 161–170.
[7] Y. Sakaguchi, I. Sekiya, K. Yagishita, T. Muneta, Comparison of human stem cells derived from various mesenchymal tissues: superiority of synovium as a cell source, Arthritis Rheum. 52 (2005) 2521–2529.
[8] A.R. Armiento, M.J. Stoddart, M. Alini, D. Eglin, Biomaterials for articular cartilage tissue engineering: learning from biology, Acta Biomater. 65 (2018) 1–20.
[9] J.U. Yoo, et al., The chondrogenic potential of human bone-marrow-derived mesenchymal progenitor cells, J. Bone Jt. Surg. 80 (1998) 1745–1757.
[10] P.D. Benya, J.D. Shaffer, Dedifferentiated chondrocytes reexpress the differentiated collagen phenotype when cultured in agarose gels, Cell 30 (1982) 215–224.
[11] K. Pelttari, et al., Premature induction of hypertrophy during in vitro chondrogenesis of human mesenchymal stem cells correlates with calcification and vascular invasion after ectopic transplantation in SCID mice, Arthritis Rheum. 54 (2006) 3254–3266.
[12] C. Scotti, et al., Recapitulation of endochondral bone formation using human adult mesenchymal stem cells as a paradigm for developmental engineering, Proc. Natl. Acad. Sci. 107 (2010) 7251–7256.
[13] K. Hjelle, E. Solheim, T. Strand, R. Muri, M. Brittberg, Articular cartilage defects in 1,000 knee arthroscopies, Arthrosc. J. Arthrosc. Relat. Surg. 18 (2002) 730–734.
[14] F. Shapiro, S. Koide, M.J. Glimcher, Cell origin and differentiation in the repair of full-thickness defects of articular cartilage, J. Bone Jt. Surg. 75 (1993) 532–553.
[15] J.A. Buckwalter, Articular cartilage injuries, Clin. Orthop. Relat. Res. 402 (2002) 21–37.
[16] R.M. Frank, E.J. Cotter, I. Nassar, B. Cole, Failure of bone marrow stimulation techniques, Sports Med. Arthrosc. 25 (2017) 2–9.
[17] P. Hernigou, A. Poignard, F. Beaujean, H. Rouard, Percutaneous autologous bone-marrow grafting for nonunions: influence of the number and concentration of progenitor cells, J. Bone Jt. Surg. - Ser. A 87 (2005) 1430–1437.
[18] L.A. Fortier, et al., Concentrated bone marrow aspirate improves full-thickness cartilage repair compared with microfracture in the equine model, J. Bone Jt. Surgery-American 92 (2010) 1927–1937.

[19] K.-Y. Saw, et al., Articular cartilage regeneration with autologous marrow aspirate and hyaluronic acid: an experimental study in a goat model, Arthrosc. J. Arthrosc. Relat. Surg. 25 (2009) 1391–1400.
[20] E. Solheim, et al., Results at 10–14 years after microfracture treatment of articular cartilage defects in the knee, Knee Surgery, Sport. Traumatol. Arthrosc. 24 (2016) 1587–1593.
[21] A. Gobbi, G. Karnatzikos, A. Kumar, Long-term results after microfracture treatment for full-thickness knee chondral lesions in athletes, Knee Surgery, Sport. Traumatol. Arthrosc. 22 (2014) 1986–1996.
[22] H. Chen, et al., Drilling and microfracture lead to different bone structure and necrosis during bone-marrow stimulation for cartilage repair, J. Orthop. Res. 27 (2009) 1432–1438.
[23] A.S. Khalil, et al., Single-dose mRNA therapy via biomaterial-mediated sequestration of overexpressed proteins, Sci. Adv. 6 (2020).
[24] A. Plaas, et al., The relationship between fibrogenic tgfβ1 signaling in the joint and cartilage degradation in post-injury osteoarthritis, Osteoarthr. Cartil. 19 (2011) 1081–1090.
[25] G. Fontana, et al., Mineral-coated microparticles enhance mRNA-based transfection of human bone marrow cells, Mol. Ther. Nucleic Acids 18 (2019).
[26] Frédéric Ceuninck, P.P. Massimo Sabatini, Cartilage and Osteoarthritis : Volume 2: Structure and in Vivo Analysis, 2004.
[27] Q. Fan, et al., Implantable blood clot loaded with BMP-2 for regulation of osteoimmunology and enhancement of bone repair, Bioact. Mater. 6 (2021) 4014–4026.
[28] G.M. Leclerc, F.R. Boockfor, W.J. Faught, L.S. Frawley, Development of a destabilized firefly luciferase enzyme for measurement of gene expression, Biotechniques 29 (2000) 590–601.
[29] A.S. Khalil, A.W. Xie, H.J. Johnson, W.L. Murphy, Sustained release and protein stabilization reduce the growth factor dosage required for human pluripotent stem cell expansion, Biomaterials 248 (2020) 120007.
[30] A.S.A.S. Khalil, et al., Functionalization of microparticles with mineral coatings enhances non-viral transfection of primary human cells, Sci. Rep. 7 (2017) 1–12.
[31] C. Lesage, et al., Material-assisted strategies for osteochondral defect repair, Adv. Sci. 9 (2022) 1–20.
[32] A.E. Sams, A.J. Nixon, Chondrocyte-laden collagen scaffolds for resurfacing extensive articular cartilage defects, Osteoarthr. Cartil. 3 (1995) 47–59.
[33] M. Maruyama, et al., Comparison of the effects of osteochondral autograft transplantation with platelet-rich plasma or platelet-rich fibrin on osteochondral defects in a rabbit model, Am. J. Sports Med. 45 (2017) 3280–3288.
[34] J.S. Fernandez-moure, et al., Platelet-rich plasma: a biomimetic approach to enhancement of surgical wound healing, J. Surg. Res. 207 (2017) 33–44.
[35] H. Chiang, C.-C. Jiang, Repair of articular cartilage defects: review and perspectives, J. Formos. Med. Assoc. 108 (2009) 87–101.
[36] A. Gobbi, M. Fishman, Platelet-rich plasma and bone marrow-derived mesenchymal stem cells in sports medicine, Sports Med. Arthrosc. 24 (2016) 69–73.
[37] P. Hernigou, A. Poignard, F. Beaujean, H. Rouard, Percutaneous autologous bone-marrow grafting for nonunions: influence of the number and concentration of progenitor cells, J. Bone Jt. Surg. - Ser. A 87 (2005) 1430–1437.
[38] A. Pascher, et al., Gene delivery to cartilage defects using coagulated bone marrow aspirate, Gene Ther. 11 (2004) 133–141.
[39] B.L. Schumacher, J.A. Block, T.M. Schmid, M.B. Aydelotte, K.E. Kuettner, A novel proteoglycan synthesized and secreted by chondrocytes of the superficial zone of articular cartilage, Arch. Biochem. Biophys. 311 (1994) 144–152.
[40] T.E. Hardingham, R.A. Oldershaw, S.R. Tew, Cartilage, SOX9 and Notch signals in chondrogenesis, J. Anat. 209 (2006) 469–480.
[41] T.N. Hissnauer, et al., Identification of molecular markers for articular cartilage, Osteoarthr. Cartil. 18 (2010) 1630–1638.
[42] X. Yu, et al., Nanostructured mineral coatings stabilize proteins for therapeutic delivery, Adv. Mater. 29 (2017) 1–9.
[43] T. Re'em, O. Tsur-Gang, S. Cohen, The effect of immobilized RGD peptide in macroporous alginate scaffolds on TGFβ1-induced chondrogenesis of human mesenchymal stem cells, Biomaterials 31 (2010) 6746–6755.
[44] P.M. van der Kraan, E.N. Blaney Davidson, A. Blom, W.B. van den Berg, TGF-beta signaling in chondrocyte terminal differentiation and osteoarthritis, Osteoarthr. Cartil. 17 (2009) 1539–1545.
[45] C.R. Chu, M. Szczodry, S. Bruno, Animal Models for Cartilage Regeneration and Repair, vol. 16, 2010.
[46] M. Youssef, C. Hitti, J. Puppin Chaves Fulber, A.A. Kamen, Enabling mRNA therapeutics: current landscape and challenges in manufacturing, Biomolecules 13 (2023) 1497.
[47] G. Fontana, et al., Mineral-coated microparticles enhance mRNA-based transfection of human bone marrow cells, Mol. Ther. Nucleic Acids 18 (2019) 455–464.